THE ROYAL SOCIETY

Correlation equations for endemic diseases: externally imposed and internally generated heterogeneity

M. J. Keeling

Department of Zoology, University of Cambridge, Downing Street, Cambridge CB2 3EJ, UK (matt@zoo.cam.ac.uk)

The simple susceptible–infectious–recovered (SIR) model has provided many insights into the behaviour of a single epidemic. However, most of epidemiology is concerned with endemic infections, and for this to occur fresh susceptibles need to be generated. This is usually provided by individuals becoming susceptible soon after birth or by recruitment to cohorts at risk. This paper develops a correlation model, predicting the behaviour of connected pairs of individuals, which includes demographic processes as well as the basic epidemiology. In addition to the local spatial correlations, we consider three other forms of heterogeneity: internally generated heterogeneity in terms of stochasticity or imposed heterogeneity in terms of non-uniform vaccination or age-structure.

Keywords: correlation equations; contact networks; spatial heterogeneity; disease persistence; power-law behaviour; vaccination

1. INTRODUCTION

It has already been shown that considering and modelling the network structure of disease transmission can have a profound effect on the dynamics of a single epidemic (Dietz & Hadeler 1988; Altmann 1995; Keeling *et al.* 1997; Keeling 1999). Modelling pairs of connected individuals provides an analytical method of determining the effects of a small, interconnected neighbourhood of contacts. In general, a small number of transmission connections and highly interconnected neighbourhoods lead to lower R_0 and a smaller final size for the epidemic (Keeling 1999). However, the majority of epidemiology is concerned with the behaviour of endemic diseases—ones which persist in a population. For a disease to persist requires the susceptibles to be replenished, so that the infection has a continual source of 'fuel'. This paper considers the case where the replenishment of susceptibles is from births into the population, as in the case of childhood diseases, although there are obvious similarities to the modelling of sexually transmitted disease where replenishment of susceptibles is due to recruitment into high-risk cohorts.

The first section introduces a new approach where the inclusion of 'virtual' empty sites allows far greater flexibility in the neighbourhoods of correlation models. The first form of externally imposed heterogeneity considered comes from the placement of new susceptibles, either at random or next to other susceptibles—approximating age structure. The next section considers external heterogeneity in the form of aggregated vaccination. To consider fully the effects of vaccination, we must understand the persistence of a disease; it is therefore imperative that the model is stochastic (Keeling 1997). The final sections consider how to include stochasticity into the correlation framework and briefly examine two well-documented measures: the distribution of epidemic sizes (Rhodes & Anderson 1996*a*,*b*) and the fade-out behaviour or persistence of epidemics (Bartlett 1956; Grenfell 1992).

2. DEMOGRAPHIC PROCESSES

Throughout this work, the notation developed in Keeling (1999) shall be used; namely, $[A]$ is the number of sites of type A, $[AB]$ is the number of A–B pairs, $[ABC]$ is the number of A–B–C triples, and $\mathcal{C}_{AB} = N[AB]/n[A][B]$ is the multiplicative correlation between A and B. The network, through which the disease spreads, is specified by three parameters: n, the number of neighbours per site; N, the number of sites; ϕ, the interconnectedness. ϕ is defined as the proportion of three connected sites which form a triangular network, it therefore measures the degree of local compared to global interaction.

To help with later comparisons, the standard susceptible–infectious–recovered (SIR) model with births and deaths will now be given.

$$\begin{aligned} \dot{S} &= -\beta\frac{SI}{\mathcal{N}} + b(S+I+R) - dS, \\ \dot{I} &= \beta\frac{SI}{\mathcal{N}} - gI - dI, \\ \dot{R} &= gI - dR. \end{aligned} \tag{1}$$

The simplest way to include births and deaths into the pairwise equations developed in Keeling (1999) would be to convert dying infectious and recovered individuals into susceptibles ones—the so-called SIRS model. This is the general approach used in many lattice-based models. However, the conversion of a recovered into a susceptible leads to an unnatural spatial structure, with susceptibles

Received 8 December 1998 *Accepted* 25 January 1999

and recovereds being highly correlated. To include the true demographic processes of birth and death, the assumption of a fixed neighbourhood size, n, needs to be relaxed. The most natural way to do this is to add another class of sites, $\emptyset$. These empty sites play no role in the epidemiology, but are occupied by a birth and created by a death.

Consider a network of N sites where each site is connected to n others, we now wish to introduce empty sites such that the ratio of neighbours to sites $(n/N = m)$ and the interconnectedness (ϕ) remain constant. We shall consider the dynamics of an infection spreading through this network in the limit where the number of empty sites tends to infinity. If we assume a multinomial form for the distribution of sites (as in Keeling 1999; see Rand (1999) for a more detailed explanation), then although the total number of connections per individual is fixed at $n(\rightarrow \infty)$, the number of neighbours that are non-empty is Poisson-distributed, with a finite mean. This variable 'neighbourhood size' is a major development from the earlier theory, and comes naturally from the infinite limit.

In this formulation, the number of non-empty sites around a given site will be highly dependent on the type of site being considered. For example, sites with many non-empty connections are likely to be infected rapidly and therefore to be in the recovered class, hence we find that recovered sites are connected to more individuals on average than susceptible sites.

Consider a system with just two species X and Y, the mean number of non-empty neighbours surrounding a site of type X is

$$\hat{n}_X = \sum_{\mathcal{Z}\neq\emptyset} \frac{[X\mathcal{Z}]}{[X]} = \frac{[XX]+[X\Upsilon]}{[X]} = m([X]\mathcal{C}_{XX} + [\Upsilon]\mathcal{C}_{X\Upsilon}).$$

Thus, the average number of non-empty neighbours is influenced by both the density of individuals and the correlation between them. Similarly, we can calculate the mean number of non-empty neighbours surrounding a non-empty site,

$$\hat{n} = \frac{\sum_{W,\mathcal{Z}\neq\emptyset} [W\mathcal{Z}]}{\sum_{W\neq\emptyset} [W]}.$$

Going from the equations for a simple epidemic (Keeling 1999) to equations which allow endemics means that the demographic processes of birth and death must be introduced. Deaths are simple to include into the pairwise equations as these just take the form of random movements into the empty class, births on the other hand need a little more consideration. We wish births to occur at a rate $B = b([S]+[I]+[R])$, therefore the rate at which an empty site becomes susceptible is $B/[\emptyset]$. We can now formulate evolution equations for the nine different pair combinations (see Appendix A).

The inclusion of demographic events means that six equations are now necessary (without demography, only five were required) as $[S]+[I]+[R]$ no longer sums to a constant, although $[S]+[I]+[R]+[\emptyset]$ does. Equation (A2) is the obvious extension to the single epidemic model (Keeling 1999) if we allow the neighbours to be Poisson-distributed (Rand 1999); the inclusion of empty sites has enabled us to approach this extension, which has a non-constant neighbourhood size, with greater rigour.

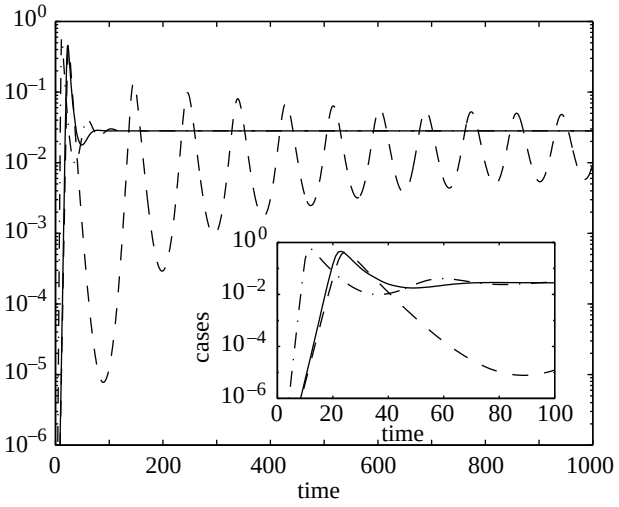

Figure 1. The time-series from the three SIR models: the mean-field equation (1), dot–dashed line; the standard correlation model (A2), dashed line; and the age-structured correlation model (2), solid line. From the main graph, we can see that the age-structured and mean-field models have the same stable fixed point, whereas the standard correlation model has an attracting limit cycle. From the inset graph, which shows the early behaviour of the three systems, we find that the two correlation models have very similar behaviour over the first 30 time intervals. $\widehat{n} = 5$, $\beta = 2.5$, $g = 0.3$, $b = d = 0.01$, $\phi = 0.4$.

It should be noticed that in the formulation given in Appendix A, a birth has equal probability of being placed in any empty site and therefore forming connections with a random cross-section of the community. However, this is usually not the case, the majority of contacts usually form between individuals of the same age or social group. As a first step towards this approach, the probability of being born into an empty site is proportional to the number of susceptibles it is connected to. This approach is ideal for childhood diseases where the majority of transmission occurs between schoolchildren who are initially all susceptible (Schenzle 1984; Bolker & Grenfell 1993). The inclusion of a strong correlation between births and susceptibles is an approximation to age structure, and modifies two terms in equation (A2) (Appendix A)

$$\begin{aligned}[\dot{SS}] &= -2\tau[SSI] + 2B(1 + m[S][1 - \phi + \phi\mathcal{C}_{SS}]) - 2d[SS],\\ [\dot{SI}] &= \tau([SSI] - [ISI] - [SI]) - g[SI]\\ &\quad + Bm[I][1 - \phi + \phi\mathcal{C}_{SI}] - 2d[SI], \end{aligned} \tag{2}$$

Figure 1 compares the time-series from the three equations (1), (A2) and (2)—the mean-field model, and the standard and age-structured pairwise models. The results shown in the graph are generic and the general forms have been checked by calculating fixed points and eigenvalues. The standard correlation model (A2) usually has a lower proportion of infectious at its fixed point than the comparative mean-field equations (1), but is far less stable, frequently giving rise to limit cycles (as seen in figure 1). By contrast, the age-structured correlation model (2) and the mean-field equations have an identical proportion of infectious at their

fixed points, although strong correlations still exist for equation (2) forming clusters of susceptibles and clusters of infectious individuals. The age-structured model is more stable than the mean-field and hence can never generate limit cycle behaviour. Upon the introduction of an infection into a population, both correlation models behave similarly in the early stages (until $t = 30$) as local scale spatial structure is formed (inset figure 1).

These results can be intuitively explained by considering the distribution of new susceptibles. For the standard correlation model, many new susceptibles are surrounded by recovered individuals and so are isolated from the disease; only when sufficient susceptibles have been born to form connections across the network (cf. percolation behaviour) can the disease progress—this leads to oscillatory dynamics. With the age-structured model, however, new births are always connected to other susceptibles and so are accessible to the disease; the births are continually refuelling the infection.

If we assume that no disease is present, so we simply have a birth–death process, then we can calculate the aggregation of susceptibles as measured by $\mathcal{C}_{SS}$. For the standard correlation model (A2) we find,

$$\frac{\mathrm{d}\mathcal{C}_{SS}}{\mathrm{d}t} = 2b(1-\mathcal{C}_{SS}) \qquad \Rightarrow \qquad \mathcal{C}_{SS} \to 1,$$

hence the susceptibles are randomly distributed and the neighbourhood sizes are Poisson, whereas, for the age-structured equations (2) we obtain,

$$\frac{\mathrm{d}\mathcal{C}_{SS}}{\mathrm{d}t} = \frac{2b}{m}[S]^2(1+m[S](1-\phi)-m[S](1-\phi)\mathcal{C}_{SS})$$
$$\Rightarrow \qquad \mathcal{C}_{SS} \to \frac{1+m[S](1-\phi)}{m[S](1-\phi)} > 1.$$

Therefore, the age-structured model leads to the aggregation of susceptibles, with there being a higher proportion of large neighbourhoods. The greatest aggregation occurs when the average number of neighbours is small, there are few susceptibles and the interconnectedness, ϕ, is large. This agrees with the numerical results for the full system.

If we also consider the SIRS system, where new susceptibles are generated from recovered individuals, then we observe greater instability than for all the other models. In a spatial framework, the conversion of recovered individuals into susceptibles means that prominent waves of infection are produced. Therefore, the waves of infection observed in many lattice-based systems may be a feature of the demography as much as the epidemiology.

The equality in the number of infectious individuals at the fixed points of equations (1) and (4), may help to explain why mean-field models have been so good at predicting the deterministic behaviour of epidemics—even when strong correlations are expected. By comparison, the different strengths of the eigenvalues indicate that systems with seasonality, high levels of stochasticity or far from the fixed point should behave very differently. In reality, we should expect the behaviour to lie somewhere between the two extremes of (A2) and (2). Which equations form the best model is dependent on the dynamics of the disease, the social structure of the population and the average age of infection. In the work that follows, the random birth model (A2) will be taken as the standard equations due to their simpler form and more generic assumptions.

3. THE DYNAMICS WITH AGGREGATED VACCINATION

We shall now extend the non-age-structured model to include vaccination. Vaccination 'moves' susceptible individuals into a new vaccinated class (V) after which they are immune to the disease. Although we shall assume a constant vaccination rate v per individual, we shall allow vaccination to be an aggregated process, i.e. the probability of being vaccinated increases with the number of vaccinated neighbours. It has long been realized that there are heterogeneities in the levels of vaccination at a variety of scales, with aggregation at the family, community and district level. We scale between random vaccination and aggregated (proportional to the number of vaccinated neighbours) with a parameter α. This leads to a set of 14 coupled ordinary differential equations which are given in Appendix B.

To gain a more intuitive understanding of the effects of α, we shall ignore the infection process, set births equal to deaths, and consider the long-term behaviour of the correlations. From the equation for $[\dot{V}]$, we find

$$[S] = \frac{b}{b+v}\mathcal{T}, \qquad [V] = \frac{v}{b+v}\mathcal{T},$$

and when $\phi = 0$,

$$\mathcal{C}_{SS} \to 1,$$
$$\mathcal{C}_{SV} \to 1 - \frac{\alpha(v+b)}{(2b+v)m\mathcal{T}} < 1,$$
$$\mathcal{C}_{VV} \to 1 + \frac{2\alpha(v+b)b}{(2b+v)m\mathcal{T}v} > 1.$$

Hence, as α becomes small, or the average number of non-empty neighbours ($\hat{n} \approx m\mathcal{T}$) is large, then the correlations decay to one. If we add some amount of interconnectedness, ϕ, then we can no longer obtain analytical solutions for the correlations, but numerical results show that $\mathcal{C}_{SS}$ and $\mathcal{C}_{VV}$ increase with ϕ, while $\mathcal{C}_{SV}$ decreases.

Returning to the full equations with infection, extensive sweeps of parameter space have shown that, at the non-trivial fixed point of equations (B1), greater aggregation (α) leads to an increase in $\mathcal{C}_{SS}$ and hence a greater level of infection. This would lead us to the conclusion that random (rather than aggregated) vaccination campaigns should be more successful at eradicating a disease—this agrees with earlier conclusions from examining the basic reproductive ratio R_0 (Keeling 1999).

However, when the full dynamics are considered, an alternative scenario is apparent. The greater the aggregation of vaccination, the more unstable the model becomes and the lower the level of the disease in the troughs between major epidemics (figure 2). Thus, although initially it appears advantageous to avoid aggregation of vaccinated individuals, the low number of cases in the troughs means that we are much more likely to

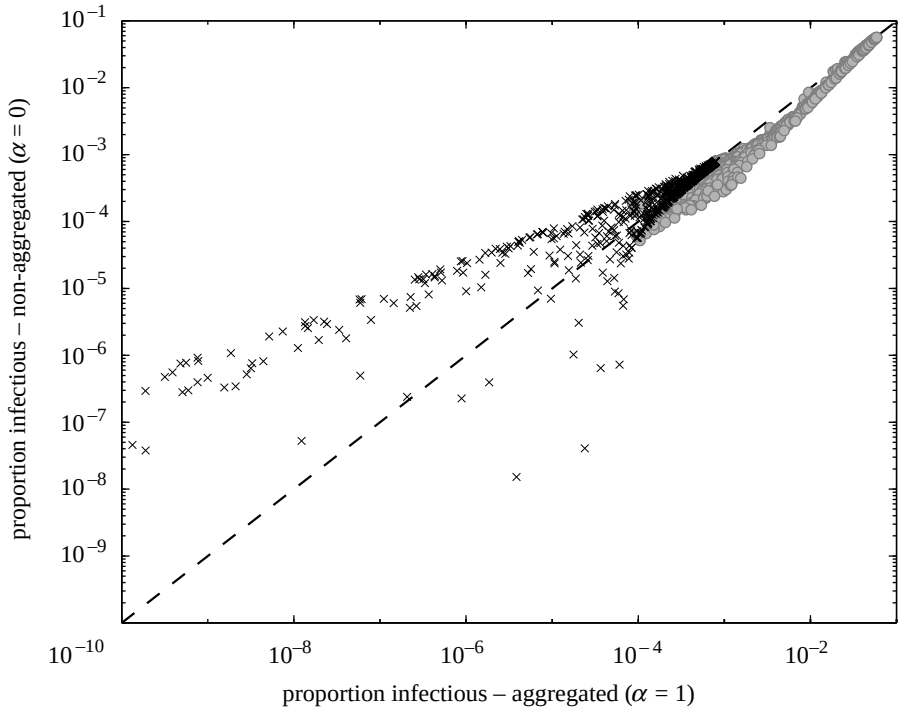

Figure 2. Although the aggregated vaccination model ($\alpha = 1$) consistently shows a larger number of cases at the fixed point, over a wide sweep of parameter space, it is generally less stable. This graph shows the maximum and minimum number of cases on the attracting periodic orbit of equation (B1) for 1000 random parameter choices. The crosses give the minimum values, which are generally less in the aggregated model; the circles give the maximum values, which are generally higher.

experience stochastic fade-out when the vaccinated individuals are clustered. This phenomenon is re-examined in § 4b with stochastic models.

4. STOCHASTIC UPDATING

To understand fully the persistence of a disease, it is necessary to allow for demographic stochasticity (cf. Bartlett 1956; Grenfell 1992; Keeling & Grenfell 1997). It has already been shown (Keeling *et al*. 1997) that stochastic pairwise models can lead to increased persistence of measles epidemics. Here, the stochastic formulation for the pairwise model will be discussed together with results for persistence and power-law behaviour. This stochastic nature introduces two related considerations: what is the distribution of neighbourhoods about a site and when an event occurs what is the distribution of pairs that are also affected?

For the case of no triangular connections ($\phi = 0$), we can predict the probability of a site of type A being surrounded by s susceptibles, i infectious and r recovereds. As we are now dealing with a finite system, forming the neighbourhood corresponds to 'drawing balls from a bag without replacement'. Considering drawing pairs that have an A at one end leads to a binomial-type distribution

$$P_A(s,i,r) = \left(\frac{[A]-1}{[A]}\right)^{[AS]+[AI]+[AR]} ([A]-1)^{-s-i-r} \times \binom{[AS]}{s}\binom{[AI]}{i}\binom{[AR]}{r}, \quad (3)$$

where $\binom{A}{B}$ is the binomial coefficient $A!/(A-B)!B!$. This probability is formed as a multinomial expression for a finite number of empty sites, before letting $n \to \infty$. When $[A] = 1$, only the probability for $s = [AS]$, $i = [AI]$ and $r = [AR]$ is non-zero. It should be noted that this probability is, at best, an approximation, as without taking into account the exact distribution of all individuals over the entire network inconsistencies can always occur.

The formulation of a stochastic model is in two parts; the time to the next event and the type of event can be calculated from the simple rates in the underlying equation, but the neighbourhood of the affected site and therefore the number of pair types affected is more complex. For example, when a susceptible centre site is infected, we should expect the neighbourhood to contain a high concentration of infectious individuals as the more infecteds in the neighbourhood the greater the chance of catching the disease.

$$\text{prob}(sir \text{ neighbourhood}) = \frac{\tau i P_S(s,i,r)\,[S]}{\tau[SI]}.$$

On the other hand, as the movement from infectious to recovered does not depend on the neighbourhood, we should assume that the number of pair-types is close to binomial.

$$\text{prob}(sir \text{ neighbourhood}) = \frac{g\,P_I(s,i,r)[I]}{g[I]}.$$

Despite the highly skewed distribution of neighbours for some events, the expected rate of change of the pairs from this stochastic process is the same as those calculated in the underlying deterministic equation.

The change from a stochastic mean-field model to a stochastic pairwise one is frequently accompanied by an increase in the variance of the dynamics. In the mean-field system, when an event occurs the rates of change alter by a fixed amount. However, for the pairwise approach, each event can be accompanied by a variety of changes to the number of pairs, hence there is some

variation in the amount by which the global rates of change alter. This, in turn, leads to greater overall variance between simulations—a result which generally holds for most true spatial models. A detailed quantitative comparison between stochastic mean-field models and stochastic pairwise models is not appropriate as the underlying deterministic systems differ so much. In general, however, it was found that a pairwise stochastic system leads to less violent epidemics and a smaller number of cases when the epidemic takes off, than its mean-field counterpart, although there is a greater chance that the epidemic will persist.

(a) *Power-law behaviour*

Demographic stochasticity is very important when considering the dynamics and persistence of an infection in small isolated communities. Owing to the stochastic nature of these systems, it is difficult to compare two epidemics, hence we wish to examine a simple statistical measure of many epidemics. One subject which has received increasing interest of late is the power-law distribution of epidemics (Rhodes & Anderson 1996*a*,*b*; Rhodes *et al*. 1997; Keeling *et al*. 1997). The power-law distribution is closely bound with ideas of spatial structure and self-organized criticality. Can the correlation models formulated here produce similar distributions?

Using standard notation, it is assumed that the number of epidemics of size s is

$$N(s) \propto s^{-\gamma+1},$$

however, to achieve a smoother graph, it is better to examine the probability, $P(s)$, that an import triggers an epidemic of size greater than or equal to s,

$$P(s) = \sum_{r=s}^{\infty} N(r) \propto s^{-\gamma+2}.$$

Plotting $P(s)$ against s on a log–log graph, the value of γ can be estimated from the gradient for small s (figure 3, inset). From a variety of parameter settings, γ was found to lie between two and three, being a monotonically decreasing function of β (figure 3). The age-structured version (equation (2)) produced similar results, but with γ slightly reduced. These predictions agree with data from the Faroe Islands (Rhodes *et al*. 1997) which predict that for measles ($R_0 \approx 12$) $\gamma \approx 2.26$, whereas for mumps, which is less contagious ($R_0 \approx 10$) and therefore has a lower contact rate (β), the exponent $\gamma \approx 2.45$.

The inset in figure 3 is a log–log plot of $P(s)$ against s when the average number of neighbours $\hat{n} = 4$, showing the initial power-law scaling with s. When β is small, such that R_0 is close to one, there is a flat plateau, caused by a lack of epidemics of sizes between 100 and 5000, this is due to the failure of many epidemics together with occasional large outbreaks. When β is large, however, although the power-law scaling is shallower, it continues into the thousands, therefore large transmissibilities cause many smaller epidemics but far fewer large ones.

(b) *The stochastic persistence of infection*

The only true way to determine the impact of vaccination is with the use of stochastic models which can predict the level of stochastic fade-out. In this section, we wish to assess the deterministic result of § 3, that aggregated infection may actually promote the eradication of a disease. The stochastic models show that the number of fade-outs within a population is determined by extinctions at two different time-scales: infections that fail to persist in the short-term (as captured by R_0) and infections that die out once they are established. For all values of ϕ, aggregated vaccination produces a higher R_0 (Keeling 1999) and therefore more infections succeed in their early stages. When ϕ is small, however, this is counteracted by more fade-outs of established infections, as the underlying differential equations are less stable for aggregated vaccination. Hence, for small ϕ (<0.2), eradication of the disease is promoted by aggregated vaccination (figure 4*a*), whereas for large ϕ the reverse is true (figure 4*b*).

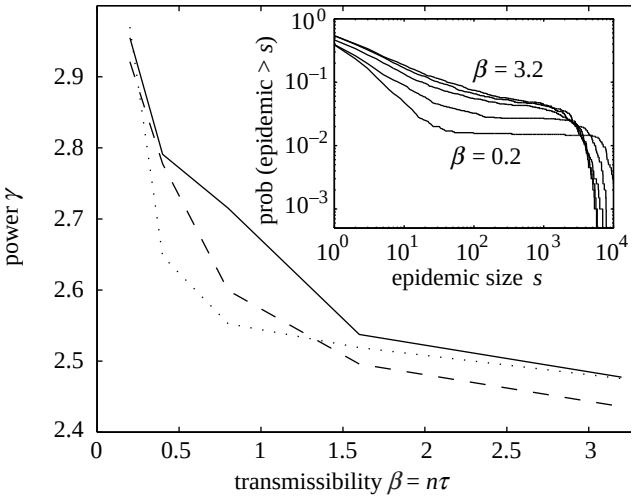

Figure 3. The power-law exponent γ against the contact rate β for a variety of neighbourhood sizes, when $g = 0.1$, $b = d = 5.5 \times 10^{-5}$, $\phi = 0$, with two imports per year and a population size of 25 000. The average numbers of non-empty neighbours $\hat{n}$ are 2 (dotted line), 4 (dashes), 8 (solid line). For $\hat{n} = 4$, the probability distribution of epidemic sizes, $P(s)$, for a range of contact rates is shown in the inset graph. Small contact rates show a characteristic plateau, larger contact rates exhibit power-law scaling over a wider range of epidemic sizes.

It is interesting to note that this model can also display a phenomenon observed in the measles data for England and Wales. For moderate levels of vaccination (around 60%, as was the case from 1970 to 1985), there was little or no change in the persistence of measles, although the overall number of cases was reduced (Keeling 1997)—it is not until the level of vaccination is much higher (around 90%) that the persistence rapidly declines. Non-spatial, stochastic models have so far been unable to capture this behaviour, although the pairwise model displays a similar response for a wide range of parameter values (figure 4*c*).

5. DISCUSSION

This paper has considered the effects of various forms of heterogeneity on simple epidemiological dynamics spread through a network of contacts. We have also shown how a more natural network with a variable number of neighbours may be included in correlation models. The addition of empty sites, Ø, has naturally led to the situation where the number of occupied neighbours

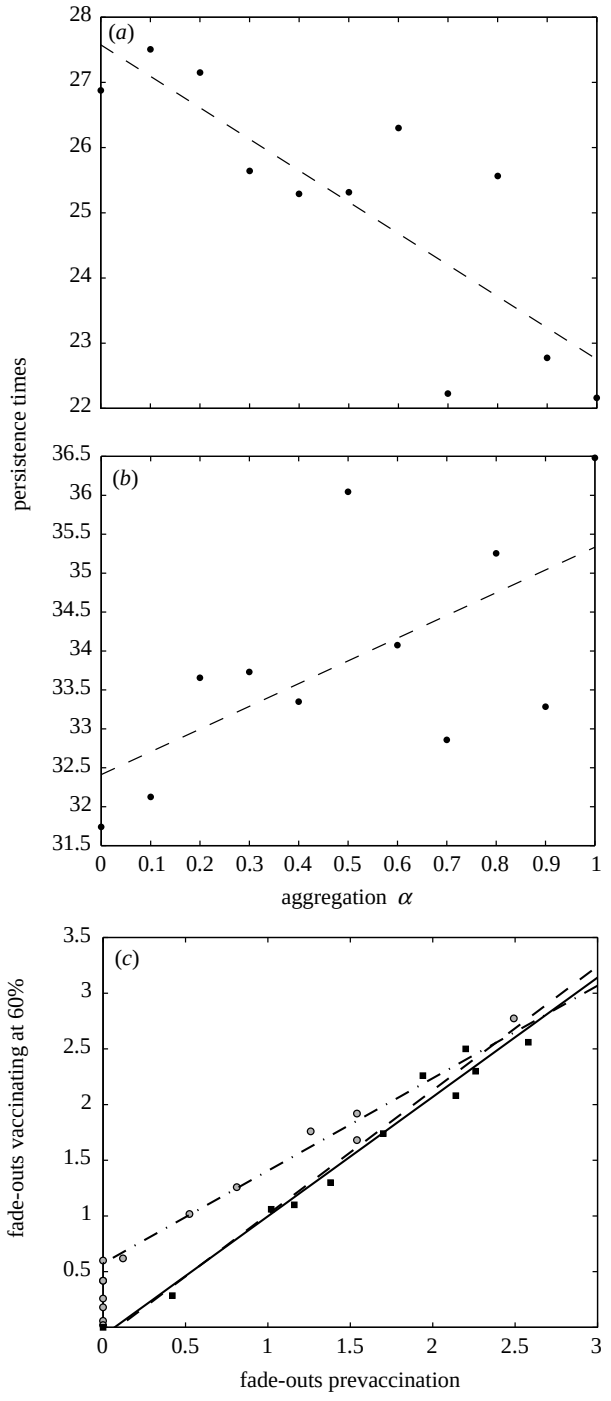

Figure 4. Results from the stochastic pairwise model, looking at how the persistence of a disease is affected by vaccination. (*a*) and (*b*) are the average persistence times for a population of 5000, when $\phi = 0$ and $\phi = 0.4$, respectively. The persistence times are an average over 1000 epidemics. When $\phi = 0$, aggregated vaccination (as measured by α) leads to a reduced persistence time and therefore more stochastic fade-outs. When $\phi = 0.4$, the situation is reversed. These relationships are very noisy but significantly different from zero ($p < 0.05$). (*c*) The average number of yearly fade-outs with 60% vaccination against the yearly fade-outs before vaccination. The solid line is a best-fit to the case reports of measles from England and Wales. The squares are the results from a pairwise model, the dashed line being the best fit. To simplify the computation, we assumed no aggregation of vaccination ($\alpha = 0$, $\hat{n} = 10$, $\tau = 0.3$, $g = 0.1$, $\phi = 0$, $b = d = 10^{-4}$). The circles are the results from a mean-field SIR model, is Poisson-distributed about a mean. This is a more realistic scenario than assuming a fixed neighbourhood size for every site. It is interesting to note that the average number of occupied neighbours about a site of type A will often vary with A—for example, after a large epidemic it will only be isolated susceptibles which have escaped infection, therefore the number of occupied neighbours around a susceptible will on average be lower. It should be realized that we have assumed that both the number of occupied neighbours and ϕ are independent of the local environment—the network structure is homogeneous. Future work aims to extend the methodology to more generalized networks.

When births are randomly distributed, the presence of local spatial correlations between susceptible and infectious individuals reduces the number of cases at equilibrium compared to the mean-field solution. However, aggregating newborn susceptibles increases the average level of infection back to the value predicted by equation (1), although the initial dynamics, after the invasion by an infection, are very different. This may indicate why mean-field models have been so successful at predicting the long-term behaviour of diseases, but have limited success when the dynamics are stochastic with large fluctuations. The age-structured model is also more stable than both the mean-field and standard pairwise equations, and cannot therefore display oscillatory dynamics. The aggregation of susceptibles breaks the wave-like spread of diseases seen in many lattice models because recovered individuals behind the wave-front are no longer converted into susceptibles.

In a similar manner, we considered the aggregation of vaccination. Earlier work (Keeling 1999) has predicted that the more aggregated the spread of vaccination, the higher the effective reproductive ratio, and that higher levels of vaccination would therefore be required to eradicate the disease. A similar conclusion would be drawn from consideration of the equilibrium point. However, examination of the full dynamics of the deterministic system shows that with greater aggregation comes greater instability of the fixed point, leading to oscillatory dynamics with low troughs between the epidemic peaks. Hence, we may find that aggregated vaccination leads to a lower persistence of the disease—this is borne out by stochastic simulations of the pairwise model which show higher levels of fade-out with aggregated vaccination. If we consider vaccination in terms of simple 'forest fire' models (Bak *et al.* 1990; Rand *et al.* 1995), then random vaccination corresponds to attempting to stop a fire by thinning out the trees, whereas aggregated vaccinationproduces large fire-breaks. 'Fire-breaks' still allow epidemics of the disease to occur ($R_0 > 1$), but these are spatially limited and quickly die out, so the level of fade-outs is far higher. When the interconnectedness ϕ is large, then aggregated vaccination produces two-dimensional 'clearings' rather

Figure 4. (*Cont.*) the dash–dot line again being a best fit—notice the higher position of the *y*-intercept indicating a smaller critical community size after vaccination ($\beta = \hat{n}\tau = 3$, $g = 0.1$, $b = d = 10^{-4}$). These results are generic for many parameter choices.

than one-dimensional 'fire-breaks' and so aggregation produces fewer fade-outs. This raises an interesting epidemiological question: should vaccination attempt to maximize stochastic fade-outs or minimize the chance of invasion (reduce R). These simple spatial models have shown that in many situations although getting a more even vaccination coverage will reduce R, it will also lead to better persistence of the disease. Therefore, if we are attempting to eradicate the disease, linear patterns of concentrated vaccination are potentially a good strategy, whereas if we are attempting to reduce the number of cases of the disease, we should attempt to get a uniform distribution of vaccine.

This research was supported by the Wellcome Trust and the Royal Society. I am indebted to David Rand for his many helpful comments, and would also like to thank Minus van Baalen, Bryan Grenfell and Odo Diekmann.

APPENDIX A

(a) *Demographic pairwise model*

$$
\begin{aligned}
[\dot{S}\dot{S}] &= -2\tau[SSI] + 2B\frac{[S\emptyset]}{[\emptyset]} - 2d[SS],\\
[\dot{S}\dot{I}] &= \tau([SSI]-[ISI]-[SI]) - g[SI] + B\frac{[I\emptyset]}{[\emptyset]} - 2d[SI],\\
[\dot{S}\dot{R}] &= -\tau[ISR] + g[SI] + B\frac{[R\emptyset]}{[\emptyset]} - 2d[SR],\\
[\dot{S}\dot{\emptyset}] &= -\tau[IS\emptyset] + B\frac{[\emptyset\emptyset]-[S\emptyset]}{[\emptyset]} + d([SS]+[SI]+[SR]-[S\emptyset]),\\
[\dot{I}\dot{I}] &= 2\tau([ISI]+[SI]) - 2g[II] - 2d[II],\\
[\dot{I}\dot{R}] &= \tau[RSI] + g([II]-[IR]) - 2d[IR],\\
[\dot{I}\dot{\emptyset}] &= \tau[IS\emptyset] + d([SI]+[II]+[IR]-[I\emptyset]),\\
[\dot{R}\dot{R}] &= g[IR] - 2d[RR],\\
[\dot{R}\dot{\emptyset}] &= d([SR]+[IR]+[RR]-[R\emptyset]),\\
[\dot{\emptyset}\dot{\emptyset}] &= 2d([S\emptyset]+[I\emptyset]+[R\emptyset]) - 2B\frac{[\emptyset\emptyset]}{[\emptyset]}.
\end{aligned}
\tag{A1}
$$

Much simplification of the above equation is possible. Because of the infinite number of empty sites, we find that there is no correlation between empty sites and any other type of site ($\mathcal{C}_{A\emptyset} = 1 \forall A$). Therefore, re-writing equation (A1) so as to eliminate terms in $\emptyset$,

$$
\begin{aligned}
[\dot{S}] &= -\tau[SI] + B - d[S],\\
[\dot{I}] &= \tau[SI] - g[I] - d[I],\\
[\dot{R}] &= g[I] - d[R],\\
[\dot{S}\dot{S}] &= -2\tau[SSI] + 2Bm[S] - 2d[SS],\\
[\dot{S}\dot{I}] &= \tau([SSI]-[ISI]-[SI]) - g[SI] + Bm[I] - 2d[SI],\\
[\dot{I}\dot{I}] &= 2\tau([ISI]+[SI]) - 2g[II] - 2d[II],\\
[\dot{R}\dot{R}] &= g[IR] - 2d[RR].
\end{aligned}
\tag{A2}
$$

APPENDIX B

(a) *Pairwise model with aggregated vaccination*

$$
\begin{aligned}
\mathcal{T} &= [S]+[I]+[R]+[V] \Rightarrow \dot{\mathcal{T}} = b\mathcal{T} - d\mathcal{T},\\
[\dot{S}] &= -\tau[SI] + b\mathcal{T} - d[S] - v[S],\\
[\dot{I}] &= \tau[SI] - g[I] - d[I],\\
[\dot{R}] &= g[I] - d[R],\\
[\dot{V}] &= v[S] - d[V],\\
[\dot{S}\dot{S}] &= -2\tau[SSI] + 2bm[S]\mathcal{T} - 2d[SS] - 2v(1-\alpha)[SS]\\
&\quad - 2v\alpha\frac{[SSV]}{[SV]}[S],\\
[\dot{S}\dot{I}] &= \tau([SSI]-[ISI]-[SI]) - g[SI] + bm[I]\mathcal{T} - 2d[SI]\\
&\quad - v(1-\alpha)[SI] - v\alpha\frac{[ISV]}{[SV]}[S],\\
[\dot{S}\dot{R}] &= -\tau[ISR] + g[SI] + bm[R]\mathcal{T} - 2d[SR]\\
&\quad - v(1-\alpha)[SR] - v\alpha\frac{[RSV]}{[SV]}[S],\\
[\dot{S}\dot{V}] &= -\tau[ISV] + bm[V]\mathcal{T} - 2d[SV] - v(1-\alpha)([SV]-[SS])\\
&\quad - v\alpha\frac{[VSV]+[SV]-[SSV]}{[SV]}[S],\\
[\dot{I}\dot{I}] &= 2\tau([ISI]+[SI]) - 2g[II] - 2d[II],\\
[\dot{I}\dot{R}] &= \tau[ISR] + g([II]-[IR]) - 2d[IR],\\
[\dot{I}\dot{V}] &= \tau[ISV] - g[IV] - 2d[IV] + v(1-\alpha)[SI]\\
&\quad + v\alpha\frac{[ISV]}{[SV]}[S],\\
[\dot{R}\dot{R}] &= g[IR] - 2d[RR],\\
[\dot{R}\dot{V}] &= g[IV] - 2d[RV] + v(1-\alpha)[SR] + v\alpha\frac{[RSV]}{[SV]}[S],\\
[\dot{V}\dot{V}] &= -2d[VV] + 2v(1-\alpha)[SV] + 2v\alpha\frac{[VSV]+[SV]}{[SV]}[S].
\end{aligned}
\tag{B1}
$$

REFERENCES

Altmann, M. 1995 Susceptible–infectious–recovered epidemic models with dynamic partnerships. *J. Math. Biol.* **33**, 661–675.

Bak, P., Chen, K. & Tang, C. 1990 A forest fire model and some thoughts on turbulence. *Phys. Lett.* A **147**, 297–300.

Bartlett, M. S. 1956 Deterministic and stochastic models for recurrent epidemics. *Proc. Third Berkley Symp. Math. Stats. Prob.* **4**, 81–108.

Bolker, B. M. & Grenfell, B. T. 1993 Chaos and biological complexity in measles dynamics. *Proc. R. Soc. Lond.* B **251**, 75–81.

Dietz, K. & Hadeler, K. P. 1988 Epidemiological models for sexually transmitted diseases. *J. Math. Biol.* **26**, 1–25.

Grenfell, B. T. 1992 Chance and chaos in measles dynamics. *J. R. Statist. Soc.* B **54**, 383–398.

Keeling, M. J. 1997 Modelling the persistence of measles. *Trends Microbiol.* **5**, 513–518.

Keeling, M. J. 1999 The effects of local spatial structure on epidemiological invasions. *Proc. R. Soc. Lond.* B **266**, 859–867.

Keeling, M. J. & Grenfell, B. T. 1997 Disease extinction and community size: modeling the persistence of measles. *Science* **275**, 65–67.

Keeling, M. J., Rand, D. A. & Morris, A. J. 1997 Correlation models for childhood epidemics. *Proc. R. Soc. Lond.* B **264**, 1149–1156.

Rand, D. A. 1999 Correlation equations for spatial ecologies. In *Advanced ecological theory* (ed. J. McGlade), pp. 99–141. London: Blackwell Scientific Publishing.

Rand, D. A., Keeling, M. J. & Wilson, H. B. 1995 Invasion, stability and evolution to criticality in spatially extended, artificial host–pathogen ecologies. *Proc. R. Soc. Lond.* B **259**, 55–63.

Rhodes, C. J. & Anderson, R. M. 1996*a* Power laws governing epidemics in isolated populations. *Nature* **381**, 600–602.

Rhodes, C. J. & Anderson, R. M. 1996*b* A scaling analysis of measles epidemics in a small population. *Phil. Trans. R. Soc. Lond.* B **351**, 1679–1688.

Rhodes, C. J., Jensen, H. J. & Anderson, R. M. 1997 On the statistical mechanics of simple epidemics. *Proc. R. Soc. Lond.* B **264**, 1639–1646.

Schenzle, D. 1984 An age-structured model of pre- and post-vaccination measles transmission. *IMA J. Math. Appl. Med. Biol.* **1**, 169–191.

As this paper exceeds the maximum length normally permitted, the author has agreed to contribute to production costs.